



ORIGINAL ARTICLE

Fumaria officinalis-assisted synthesis of Manganese nanoparticles as an anti-human gastric cancer agent



Chunfeng Li ^a, Yongle Zhang ^a, Man Li ^b, Hongfeng Zhang ^a, Ziyu Zhu ^a, Yingwei Xue ^{a,*}

^a Gastrointestinal Surgical Ward, Harbin Medical University Cancer Hospital, Harbin 150081, Heilongjiang, China

^b Department of Endoscopy, Harbin Medical University Cancer Hospital, Harbin, Heilongjiang 150081, China

Received 11 May 2021; accepted 4 July 2021

Available online 14 July 2021

KEYWORDS

Gastric cancer;
Cell viability;
Fumaria officinalis;
Mn nanoparticles

Abstract Regarding applicative, facile, green chemical research, a bio-inspired approach is being reported for the synthesis of Mn nanoparticles by *Fumaria officinalis* as a natural reducing/stabilizing and solid support agent without using any toxic and harmful reagent. The MnNPs were synthesized using an aqueous extract of *Fumaria officinalis*. The formation and morphology of the nanoparticles were evaluated using different techniques including fourier-transform infrared spectroscopy (FTIR), UV-Visible spectroscopy, X-ray diffraction analysis (XRD), scanning electron microscope (SEM), and energy dispersive X-ray analysis (EDX) analysis. The properties of *Fumaria officinalis* leaf aqueous extract and MnNPs against common human gastric cancer cell lines i.e. KATOIII, NCI-N87, and SNU-16 were studied. The results show the successful formation of MnNPs with a spherical morphology with an average size of 50.05 nm. The viability of malignant human gastric cell line reduced dose-dependently in the presence of *Fumaria officinalis* leaf aqueous extract and MnNPs. After the clinical study, MnNPs can be utilized as an efficient drug in the treatment of human gastric cancer in humans.

© 2021 Published by Elsevier B.V. on behalf of King Saud University. This is an open access article under the CC BY-NC-ND license (<http://creativecommons.org/licenses/by-nc-nd/4.0/>).

1. Introduction

Gastric cancer is one of the most common cancers in the world. The incidence of gastric cancer is increasing in urban areas and industrialized countries, as well as in countries that are experiencing economic transition, such as Eastern Europe, most Asian countries, and some South American countries. Early detection of gastric cancer is very important in improving its treatment methods. At present, the diagnosis and treatment of gastric cancer are usually based on changes in cells and tissues, which can be done with a doctor's clinical examination or conventional imaging techniques. Scientists are trying to

* Corresponding author.

E-mail addresses: xueyingwei_1234@sina.com, xueyingwei@hrbmu.edu.cn (Y. Xue).

Peer review under responsibility of King Saud University.



identify and treat gastric cancer with the first molecular changes. Nanotechnology is very suitable for detecting molecular changes (Mao et al., 2016; De Jong and Borm, 2008; Borm et al., 2006; Stapleton and Nurkiewicz, 2014).

Nanotechnology is one of the most modern technologies in the world that has unique characteristics and applications in all fields of science and technology. The nanometer is a very small unit for measuring length, used in atomic and molecular dimensions. In general, nanotechnology is the science of arranging atoms to form new molecular structures and create new materials (Mao et al., 2016; De Jong and Borm, 2008; Borm et al., 2006). Since almost all the achievements of human progress have been crystallized in the form of materials around her, nanotechnology can be applied in all fields (Patra et al., 2018; Kiasat et al., 2013). Nanotechnology does not only mean that products can be made in nanoscale, but nanotechnology is essentially the potential to act at the molecular level from atom to atom to make large, completely new molecules with the molecular organization. This science refers to systems and materials whose structure and components show new and better physical, chemical, and biological properties due to their nanometer dimensions (Stapleton and Nurkiewicz, 2014; Patra et al., 2018; Kiasat et al., 2013; Celardo et al., 2011). The purpose of nanotechnology development is to exploit the mentioned aspects through atomic, molecular, extra molecular control and to learn how to make and produce efficiently and use these devices, maintaining the stability and integration of nanostructures, and producing devices on a much larger scale. In nanomedicine, nanotechnology tools will allow physicians to perform their experiments without altering tissues or cells (Celardo et al., 2011; Arunachalam et al., 2003). Reducing the size of the test tools makes the tests faster and cheaper. One of these tools is a cantilever, which will be effective in diagnosing cancer (Celardo et al., 2011; Arunachalam et al., 2003; Liu et al., 2014; Andersson Trojer et al., 2013; You et al., 2012). One of the challenges in diagnosing cancer is detecting circulating cancer cells, in this connection, magnetic nanoparticles are used to screen, detect, and determine the severity and trace of circulating cancer cells (Andersson Trojer et al., 2013; You et al., 2012; Itani and Al Faraj, 2019; Guilbert et al., 1996; Miller and Krochta, 1997).

The use of nanoparticles in the food, electronics, and medical industries is expanding. The preparation of nanoparticle particles raises the surface area and enhances the possibility of reacting with inorganic and organic molecules (Mao et al., 2016; De Jong and Borm, 2008; Borm et al., 2006; Stapleton and Nurkiewicz, 2014). The application of nanotechnology in medicine uses very small particles in the field of treatment and diagnosis of human cancers, which has led to the creation of a modern branch of science in oncology well-known nano oncology (Patra et al., 2018; Kiasat et al., 2013; Celardo et al., 2011). Metallic nanoparticles have expanded rapidly to image tumors, show cancer biomolecules or biomarkers, and target drug delivery. Stabilization of chemotherapeutic drugs, especially enzymatic ones, in polymer nanoparticles, leads to an increase in their stability against proteases, pH, heat, and other destructive agents of their structure (Mao et al., 2016; De Jong and Borm, 2008; Borm et al., 2006; Stapleton and Nurkiewicz, 2014; Patra et al., 2018). Conductor Semi Nonocrystals Fluorescent nanocrystals, such as quantum particles conjugated to antibodies, mark and determine the exact amount of them in the tumor. Cantilever Nano and Probes

Nano and nanoparticles conjugated with particular ligands have also been studied in peripheral metastasis (Mi, 2005; Ahmad et al., 2011; Thi and Nguyen, 2016). It has been shown that nanoparticles conjugated with a metal nucleus and magnetic super strength with biological antibodies against the ERBB2 gene, at the same time, can be useful in imaging and treating cancer (Celardo et al., 2011; Arunachalam et al., 2003; Liu et al., 2014; Andersson Trojer et al., 2013). In recent years, the development of nanotechnology has led to the use of nanoparticles in various fields of electronics, optical devices, industry, biosensors, photography, production of consumer products such as sunscreens, cosmetics and sports equipment, disease diagnosis, drug delivery, and formulation of chemotherapeutic drugs (Andersson Trojer et al., 2013; You et al., 2012; Itani and Al Faraj, 2019).

Fumaria officinalis is an annual leafy plant, belongs to Fumariaceae family. The plant is known by the common name of Fumitory. *Fumaria officinalis* has various phytotherapeutic usages in traditional medicines around the world. The plant is used as a remedy to treat gastrointestinal diseases, cancer, and skin disorders (Adham et al., 2021; Sharef et al., 2020). So far, different research groups have examined the applications of *Fumaria officinalis* extract in various biological activities such as antimicrobial, anticancer, antioxidant, and antispasmodic activity (Sharef et al., 2020; Petruczynik et al., 2019). Phenolic, flavonoid, carbohydrates, glycosides, tannins, and saponins compounds are found in *Fumaria officinalis*, however, alkaloids are the predominant component in the plant. Protopine, sanquinarine, fumaritine are the main alkaloids in the plant (Adham et al., 2021; Sharef et al., 2020; Petruczynik et al., 2019; Cakić et al., 2018; Golchinvaafa et al., 2020). In the recent study, the properties of green synthesized of MnNPs using *Fumaria officinalis* leaves extract against common human gastric cancer cell lines i.e. KATOIII, NCI-N87, and SNU-16 were evaluated.

2. Experimental

2.1. Materials

The chemicals required for catalyst synthesis and catalyst applications were purchased from Sigma Aldrich.

2.2. Preparation and extraction of aqueous extract

In the new research, to prepare the plant extract, 1 L of boiling water was added to 1200 g of the dried *F. officinalis* leaves. The container was kept at room temperature for 4 h. Then, the extract was filtered using a filter paper and evaporated until to obtain the brown crude extract. A freeze dryer was applied to powder the extract.

2.3. Green synthesis and chemical characterization of MnNPs

According to the earlier researches through some modifications, the green-synthesis of MnNPs was performed (Mahdavi et al., 2020). First, 10 mL of lemon juice was added to 30 mL of $\text{MnSO}_4 \cdot \text{H}_2\text{O}$ (0.1 M) to adjust the pH at 4. Then, 20 mL of extract solution (1 g in 50 mL water) was added to

the flask and stirred for one hour at 60 °C. During the reaction time, the yellow color was changed to light brown. After that, a centrifuge at 12000 rpm for 10 min. was applied to separate the precipitate. The obtained MnNPs were put in an oven to dry at 50 °C.

2.4. Antioxidant activities of MnNPs

The free radical scavenging test was first performed by Blois in 1958, and after some modification by numerous studies in its current form. DPPH method is one of the most widely used methods for estimating antioxidant content. DPPH is a stable radical that reacts with hydrogen atom compounds. This test is based on the inhibition of DPPH, which causes the decolorization of DPPH solution by adding radical species or antioxidants. DPPH changes color from purple to yellow by taking an electron from the antioxidant compound. The free radicals in DPPH are adsorbed at 517 nm, which follows Beer Lambert's law, and decreased absorption is linearly related to the amount of antioxidants; the higher the amount of antioxidants, the more DPPH is consumed and the more purple turns yellow (Lu et al., 2021).

This experiment was performed with few changes in the method of Lu et al (Lu et al., 2021). 0.5 mL of 0.1 mM DPPH solution prepared in 95% ethanol was mixed with 100 µl of MnNPs. The resulting solution was kept in the dark at 38 °C for 31 min. The absorbance of the samples was then read at 518 nm. To compare the activity of MnNPs, standard BHT compound was used as a standard antioxidant (Lu et al., 2021).

To determine the amount of IC₅₀ (IC₅₀ is defined as the concentration required to inhibit 50% of the antioxidant activity) for MnNPs, experiments were performed at eleven different concentrations of the desired nanoparticle solution and BHT. Each experiment was performed in three shifts and the mean values were calculated. Percentage of radicalization activity was calculated through the following equation (Lu et al., 2021):

$$\text{Inhibition (\%)} = \frac{\text{Sample A.}}{\text{Control A.}} \times 100$$

In this regard, the blank adsorption indicates the adsorption of the control solution, which contains 0.5 mL of DMPH solution and 100 µl of 95% ethanol instead of MnNPs solution and adsorption of the reaction indicates the adsorption of the solution content of the MnNPs sample (Lu et al., 2021).

2.5. Anti-gastric cancer properties of MnNPs

In this study, common human gastric cancer cell lines i.e. KATOIII, NCI-N87, and SNU-16 were used to evaluate the anticancer effect of MnNPs on cell culture. For this purpose, each cell line was placed separately in T25 flasks with a complete culture medium (including DMEM (Dulbecco's Modified Eagle Medium, 10% complementary bovine fetal serum, and 1% penicillin-streptomycin solution) and at 37 °C in the incubator, cell culture was incubated with 5% CO₂.

After obtaining 80% cell density, the sample was exposed to 1% trypsin-EDTA solution and after 3 min of incubation at 37 °C in a cell culture incubator with 5% CO₂ and observation of cells removed from the bottom of the plate, the sample

was centrifuged at 5000 rpm for 5 min and then the cell precipitate was decrypted by adding trypsin culture medium. Then, the cell suspensions after adding trypan blue dye were counted by neobar slide, and cytotoxicity test was performed by MTT method. For this purpose, in each well of 96 cell culture plates, 10 µl KATOIII, NCI-N87, and SNU-16 cells were introduced with 200 µl from the complete cell culture medium, and to achieve the cell monolayer density, the plate was re-exposed to 5% CO₂ at 37 °C. After reaching 80% cell growth, the culture medium was removed and the cell surface was first washed with PBS buffer, again, in all wells, a complete two-concentration culture medium of 100 µl was introduced and 100 µl of a solution of MnNPs dissolved in PBS (mg/mL₂) was introduced into well No. 1. After mixing the nanoparticles in the culture medium, 100 µl of it was removed and added to the second well. In the next step, 100 µl of the second well was removed after stirring the medium and added to well 3. This operation was performed up to well 11 and thus the amount of nanoparticles in each well was halved, respectively. Well No. 12 contained only one cell and complete culture medium of one concentration and remained as a control. The plate was again exposed to 5% CO₂ at 37 °C for 24 h and after 24 h the cytotoxicity was determined using tetrazolium dye. 10 µl of tetrazolium dye (5 mg/ml) was added to all wells, including the control, and the plate was exposed to 5% CO₂ at 37 °C for 2 h. The dye was then removed from the wells and 100 µl of DMSO (Dimethyl sulfoxide) was added to the wells, the plate was wrapped in aluminum foil and shaken thoroughly in a shaker for 20 min. Finally, cell survival was recorded in ELISA reader at 540 nm (Lu et al., 2021):

$$\text{Cell viability (\%)} = \frac{\text{Sample A.}}{\text{Control A.}} \times 100$$

Then, based on the absorption rate of each well and its comparison with the control, the inhibitory concentration of 50% (IC₅₀) was obtained (Lu et al., 2021).

After collecting data, Minitab statistical software was used for statistical analysis. Evaluation of antioxidant results in a completely randomized design and comparison of means was Duncan post-hoc test with a maximum error of 5%. To measure the percentage of cell survival in factorial experiments with the original design of completely randomized blocks and compare the means, Duncan post-hoc test with a maximum error of 5% was used. The 50% cytotoxicity (IC₅₀) and 50% free radical scavenging (IC₅₀) were estimated with ED50 plus software (INER, V: 1.0). Measurements were reported as mean ± standard deviation.

3. Results and discussion

Common cancer treatments, including chemotherapy, radiation and surgery, may reduce the size of the tumor, but the effect of these methods is transient and has no positive effect on patient survival (Yang et al., 2011; Xinli, 2012; Allen, 2002; Byrne et al., 2008; Gao et al., 2015). Therefore, replacing more effective, more specific therapies with fewer side effects with higher anti-cancer activity is a dominant issue in clinical oncology (Byrne et al., 2008; Gao et al., 2015; Mohammed et al., 2016; Li and G F., 2014; Torchilin, 2007).

The gradual maturation of nanotechnology has been considered not only for treating cancer but also for a wide variety

of applications, especially for drug delivery and diagnostic and imaging cases. There are many types of nanoparticles available and choosing the right carriers according to demand is a key issue (Torchilin, 2007; Deshpande et al., 2013; Zhang et al., 2014; Gao et al., 2002). Nanoparticles are very close in size to biological molecules in terms of size and can easily penetrate into the cell, for this reason, one of the goals of nanotechnology is to mount molecules and drugs on nanoparticles and transfer them to the target cell (Torchilin, 2007; Deshpande et al., 2013; Zhang et al., 2014; Gao et al., 2002). It is also possible to create different surface properties for nanoparticles by attaching protective ligands to increase the nanoparticles' resistance to the immune system and increase their presence in the bloodstream, and even binding ligands to specifically bind the nanoparticles to the target tissue (Zhang et al., 2014; Gao et al., 2002; Davis et al., 2008; Matsumura et al., 2004; Nie et al., 2007).

3.1. Antioxidant properties of MnNPs

In this study, we assessed the antioxidant properties of MnNPs by using the DPPH test as a common free radical. Free radicals are atoms, molecules, or ions with unpaired electrons and are therefore very active, unstable, and highly reactive. Free radicals are formed by breaking a bond of a stable molecule. Free radicals collide with other molecules to achieve stability and can separate electrons from them, as a result, they form a chain of more unstable molecules. A free radical can have a positive, negative, or neutral charge (Namvar et al., 2014; Sankar et al., 2014; Beheshtkhoo et al., 2018). During the body's natural metabolism or under conditions such as smoking, pollution, the entry of unnecessary chemicals into the body in any way, radiation, and stress in the body produce free radicals. The most important free radical in the human body is oxygen, which can damage DNA and other molecules. Oxidative stress is the victory of free radicals over the body's antioxidant defense and is a biological attack on the body (Lu et al., 2021; Radini et al., 2018).

Antioxidants are molecules that can donate an electron to a free radical without destabilizing themselves. This stabilizes the free radical and makes it less reactive. The result of oxidative stress in the body is various degeneration, eye damage, premature aging, muscle problems, brain damage, heart failure, diabetes, cancer, and overall weakness of the immune system (Katata-Seru et al., 2018; Sangami and Manu, 2017). Oxygen radicals are continuously produced in all living organisms and with destructive effects, lead to cell damage and death. The production of oxidant species under physiological conditions has a controlled rate, but this production increases under oxidative conditions (Namvar et al., 2014; Sankar et al., 2014; Beheshtkhoo et al., 2018; Radini et al., 2018). Various studies have shown that metallic nanoparticles have very significant anti-cancer effects with omitting the free radicals (Beheshtkhoo et al., 2018; Radini et al., 2018; Katata-Seru et al., 2018; Sangami and Manu, 2017).

The scavenging capacity of MnNPs and BHT at different concentrations expressed as percentage inhibition has been indicated in Fig. 7. In the antioxidant test, the IC₅₀ of MnNPs and BHT against DPPH free radicals were 148 and 100 µg/mL, respectively (Table 1 and Fig. 1).

Table 1 The IC₅₀ of *Fumaria officinalis* (FO), MnNPs, and BHT in antioxidant test.

	FO (µg/mL)	MnNPs (µg/mL)	BHT (µg/mL)
IC ₅₀ against DPPH	404 ± 0 ^b	148 ± 0 ^a	100 ± 0 ^a

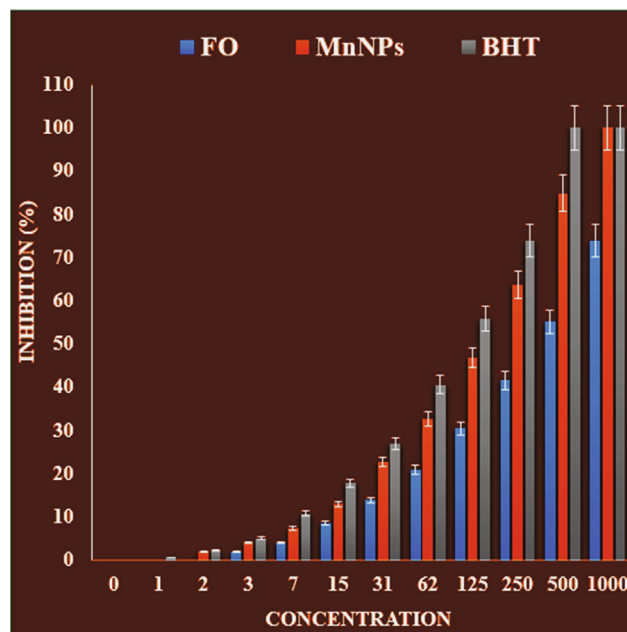


Fig. 1 The antioxidant properties of *Fumaria officinalis* (FO), MnNPs, and BHT against DPPH.

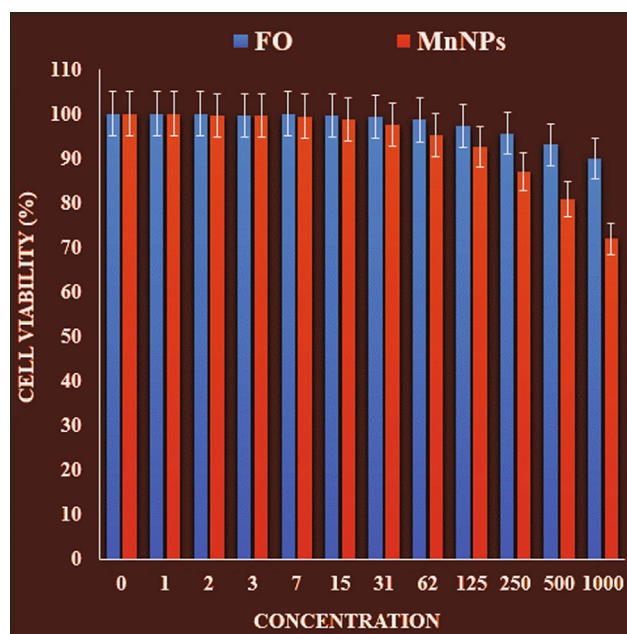


Fig. 2 The cytotoxicity effects of *Fumaria officinalis* (FO) and MnNPs against normal cell line.

3.2. Anti-gastric cancer effects analysis of MnNPs

One of the cytotoxicity test methods to measure the rate of cell death is the MTT method, which is based on the formation of formazan dye by reducing the substance MTT (dimethyl thiazole 2 and 5 diphenyltetrazolium bromide) or other tetrazolium salts (Lu et al., 2021). By breaking the MTT tetrazolium ring by mitochondrial enzymes in living cells, insoluble purple formazan crystals are formed. The formation of these crystals indicates the activity of respiratory chain enzymes and is a measure of cell viability. By measuring the amount of absorption by spectrophotometer at specific wavelengths, the number of living cells can be determined. This test is performed according to ISO 10993-5 and its purpose is in vitro evaluation of cytotoxicity. Cytotoxicity test is performed according to ISO10993-5 standard and in three ways: NRU test, CFU test, MTT test,

and XTT test. The most common method for assessing cytotoxicity is to measure cell survival by MTT (Lu et al., 2021). The basis of MTT method is based on the intensity of dye produced by the mitochondrial activity of cells, that measured at a wavelength of 540 to 630 nm and directly proportional to the number of living cells, the increase or decrease in the number of living cells is linearly related to the activity of cell mitochondria. MTT tetrazolium dye is revived inactive (metabolically) cells. Mitochondrial dehydrogenases in living cells produce NADH and NADPH, leading to an insoluble purple precipitate called formazan. This precipitate can be dissolved by isopropanol or dimethyl sulfoxide (Adham et al., 2021). Dead cells, on the other hand, are unable to perform this conversion due to the inactivity of their mitochondria and therefore do not show a signal. In this method, dye formation is used as a marker for the presence of living cells. In recent years, MTT testing has

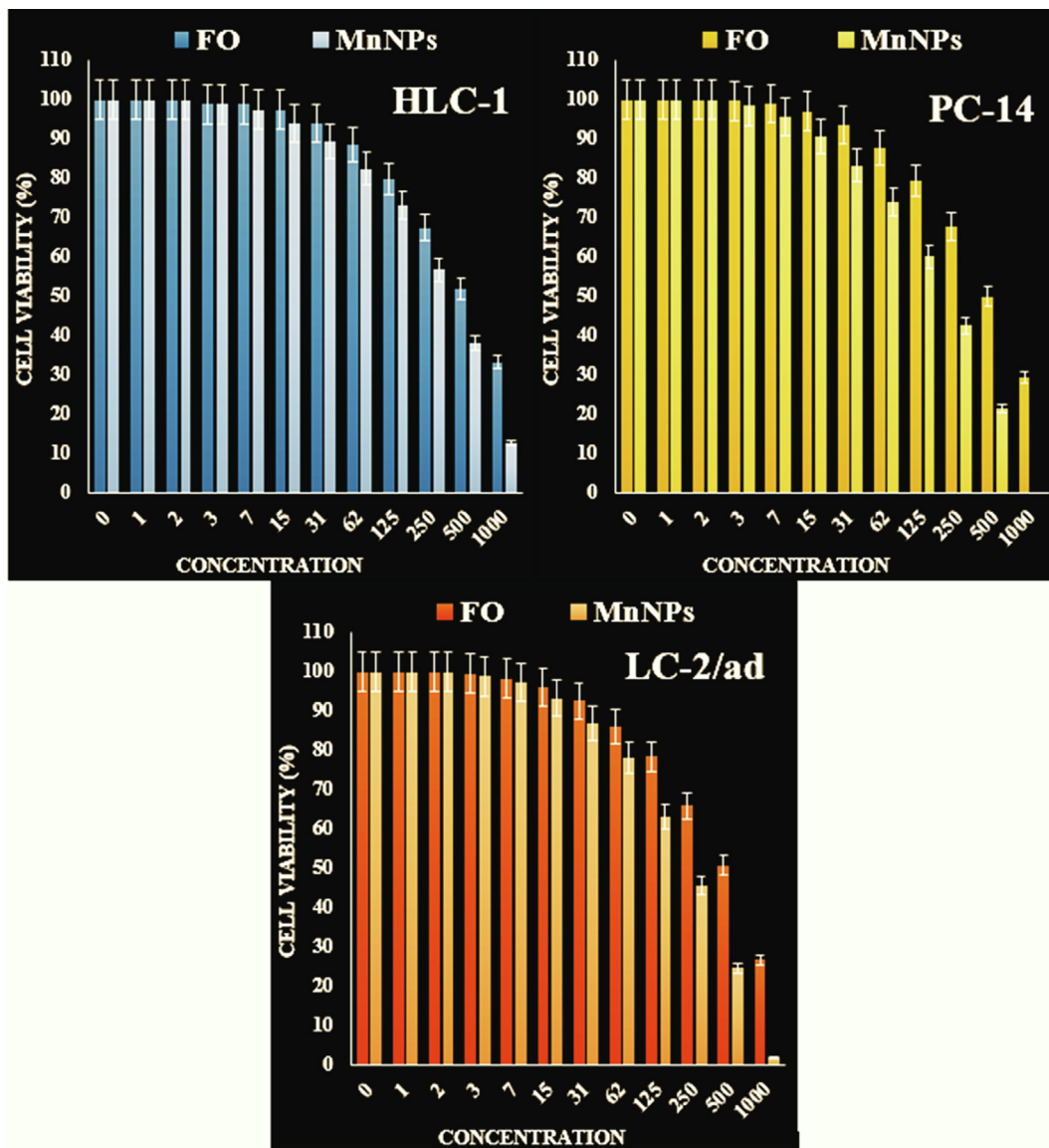


Fig. 3 The anti-human gastric cancer properties of *Fumaria officinalis* (FO) and MnNPs against gastric cancer cell lines.

Table 2 The IC₅₀ of *Fumaria officinalis* (FO) and MnNPs in the anti-human gastric cancer test.

	FO (μg/mL)	MnNPs (μg/mL)
IC ₅₀ against HUVEC	–	–
IC ₅₀ against KATOIII	553 ± 0 ^c	341 ± 0 ^b
IC ₅₀ against NCI-N87	502 ± 0 ^c	197 ± 0 ^a
IC ₅₀ against SNU-16	518 ± 0 ^c	219 ± 0 ^a

been the most important measurement method to evaluate the toxicity and anti-cancer effects of metal nanoparticles (Lu et al., 2021).

It seems that the anti-human gastric cancer effect of recent nanoparticles is due to their antioxidant effects. Because tumor progression is so closely linked to inflammation and oxidative stress, a compound with anti-inflammatory or antioxidant properties can be an anticarcinogenic agent (Nie et al., 2007; Namvar et al., 2014). Many nanoparticles have pharmacological and biochemical properties, including antioxidant and anti-inflammatory properties, which appear to be involved in anticarcinogenic and antimutagenic activities (Namvar et al., 2014; Sankar et al., 2014; Beheshtkhoo et al., 2018). Today, nanoparticles synthesized by biological methods play a vital role in treating many diseases, including cancer (Radini et al., 2018; Katata-Seru et al., 2018). Nanoparticles synthesized by biological methods are no longer the only ones in tra-

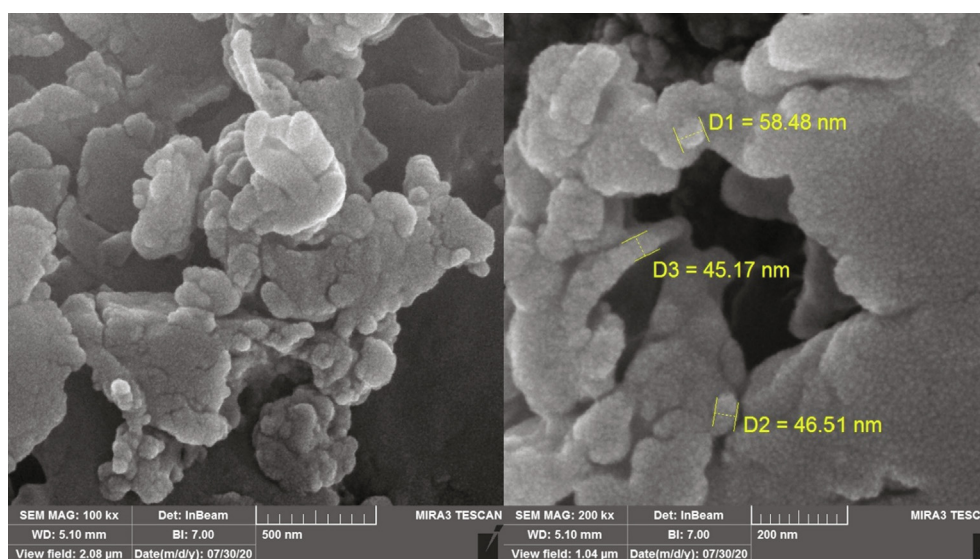


Fig. 4 SEM Images of MnNPs.

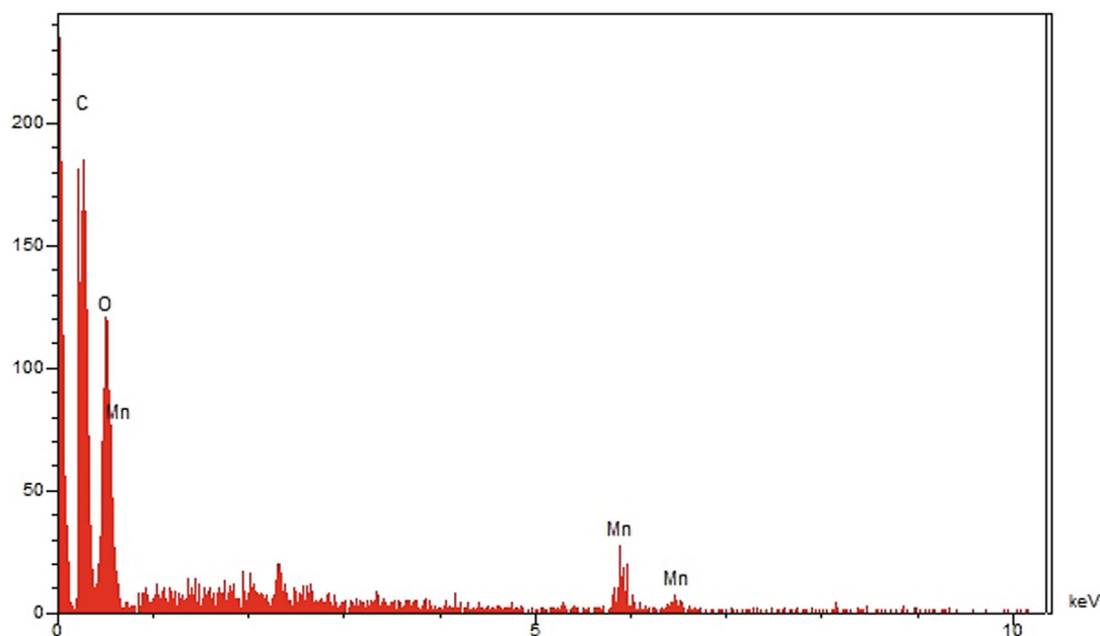


Fig. 5 EDS analysis of MnNPs.

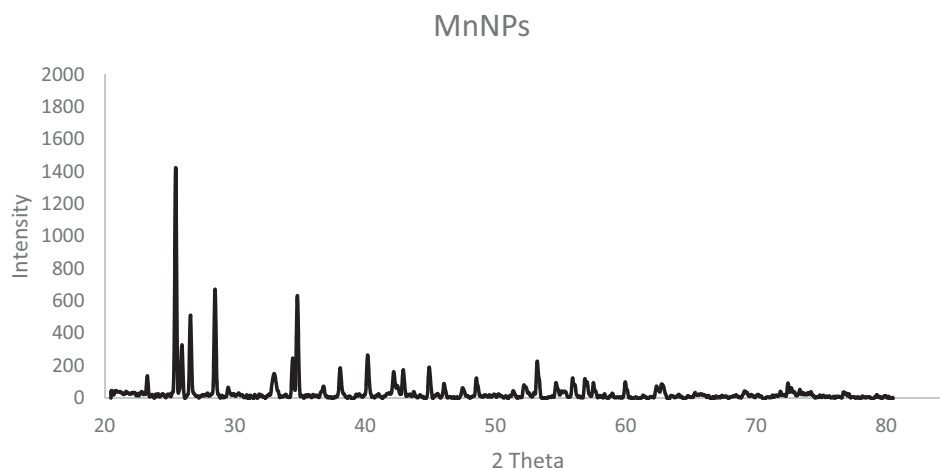


Fig. 6 XRD pattern of MnNPs.

ditional medicine, in addition, they have been able to adopt an industrial line of natural products for treating various cancers. Various cell lines from cancers of the prostate, ovary, lung, liver, and pancreas have been treated with metallic nanoparticles (Radini et al., 2018; Katata-Seru et al., 2018; Sangami and Manu, 2017).

In this investigation, the treated cells with different concentrations of the present MnNPs were assessed by MTT assay for 48 h about the cytotoxicity properties on normal (HUVEC) and human gastric malignancy cell lines i.e. KATOIII, NCI-N87, and SNU-16 (Figs. 2 and 3).

The absorbance rate was evaluated at 570 nm, which represented viability on normal cell line (HUVEC) even up to 1000 $\mu\text{g}/\text{mL}$ for MnNPs (Table 2 and Fig. 2).

The viability of malignant gastric cell line reduced dose-dependently in the presence of MnNPs.

The IC₅₀ of MnNPs were 341, 197, and 219 $\mu\text{g}/\text{mL}$ against KATOIII, NCI-N87, and SNU-16 cell lines, respectively (Table 2 and Fig. 3).

3.3. Chemical characterization of MnNPs

3.3.1. SEM and EDS analysis

The morphology of the surface and size of MnNPs was evaluated by FE-SEM technique (Fig. 4). The green-synthesized MnNPs were found in a spherical morphology with an average size of 50.05 nm. A tendency for accumulation of the synthetic nanoparticles and changeable size was approved by these images.

The EDS analysis of MnNPs, as qualitative analysis, is presented in Fig. 5. The signals at 0.52 Kev (for MnL α), 5.93 Kev (MnK α), and peak around 6.5 Kev (for MnK β) confirm the presence of manganese. In addition, the signals around 0.5 and 0.3 Kev for OK α and CK α improve the presence of oxygen and carbon in the sample.

3.3.2. XRD analysis

The XRD diffraction patterns of MnNPs evaluated its crystallinity. The pattern of the diffractogram is showed in

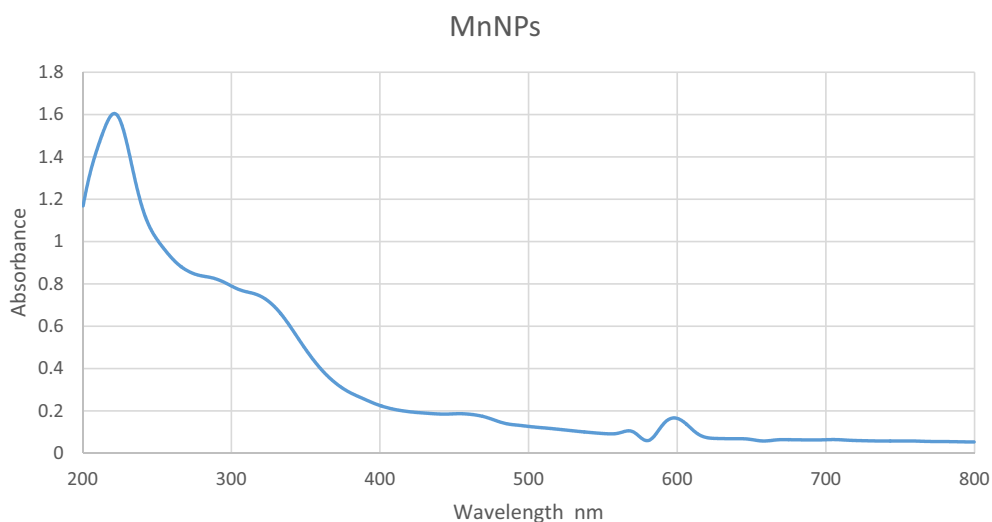


Fig. 7 UV-Visible spectrum of MnNPs.

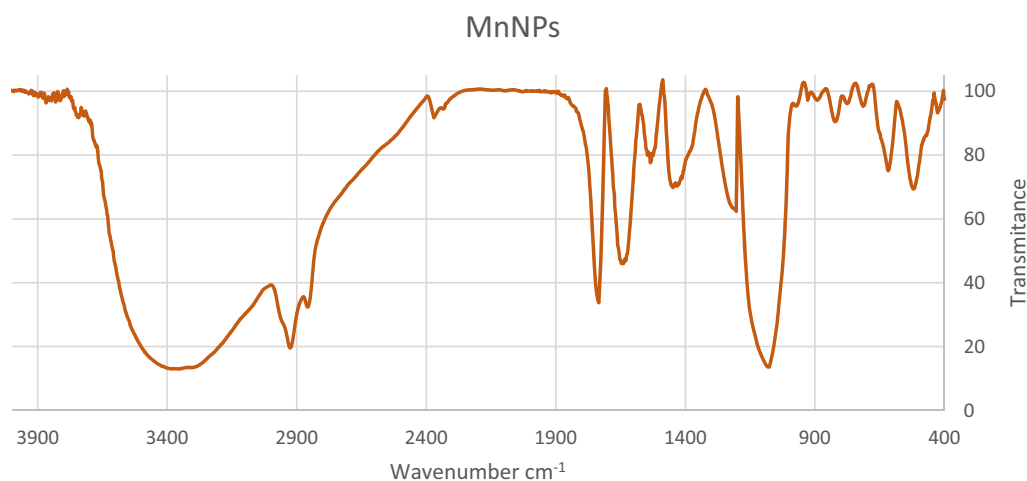


Fig. 8 FT-IR spectrum of MnNPs.

Fig. 6. The creation of manganese nanoparticles was approved for this result. Despite the small size of MnNPs, the pattern of XRD indicated well crystallizing. The achieved data were compared with the usual database of ICDD PDF card no.01-071-4929. The peaks at 28.48, 34.83, 40.25, 44.97, 53.26, 60.00 and 72.69 corresponding to MnNPs (220), (222), (400), (420), (510), (440) and (444) diffraction planes, indicate the formation of MnNPs. The peaks at diverse degrees are also reported previously (Kamran et al., 2019).

3.3.3. *Uv-Vis. spectroscopy*

The UV-Visible spectrum of the biosynthetic nanoparticles of manganese is shown in Fig. 7. The surface plasmon resonance (SPR) of MnNPs was completed using UV-Vis. spectroscopy. The creation of the biosynthetic MnNPs was observed. There was an advanced SPR band appearance at the wavelength range of 221 and 289 nm that approved the creation of MnNPs. In differentiation with a former report, the presence of the mentioned band proves the formation of manganese nanoparticles (Souri et al., 2019).

3.3.4. *FT-IR analysis*

In FT-IR spectra of the green-synthetic metallic nanoparticles, there is a region of absorption ($400\text{--}700\text{ cm}^{-1}$) that is related to metal-oxygen vibration. In the FT-IR spectrum of MnNPs Fig. 8, the peaks at 514 and 609 cm^{-1} confirm the formation of MnNPs (Mahdavi et al., 2020). On the other hand, it is obvious that many organic molecules of the extract strongly linked to Mn NPs within the synthesis step. The presence of organic compound on MnNPs is approved by the bands at different wavenumber in the FT-IR spectrum such as bands at 3417 and 2921 cm^{-1} for vibration of O—H and C—H; bands at 1448 to 1735 for C=C and C=O; and bands at 1203 and 1074 for C—O. These peaks are attributed to functional groups in an organic compound such as alkaloids, carbohydrates, phenolic compounds, flavonoids, glycosides, terpenoids, which have been found in *Fumaria officinalis* (Adham et al., 2021; Sharef et al., 2020; Petruczynik et al., 2019).

4. Conclusion

The last decade has seen the promising emergence of nanoparticles in cancer treatment systems such as drug delivery and recombinant proteins with anti-tumor properties. Special features of the microenvironment around the tumor allow nanoscale systems to accumulate at the tumor site. In the present study, the nanoparticles of manganese were synthesized by a green approach using *Fumaria officinalis* extract. The formation of MnNPs was confirmed by different chemical techniques. A 50.05 nm was measured for the particle size of the MnNPs that is a sufficient size for particles in the nanotechnology field. The viability of malignant gastric cell line reduced dose-dependently in the presence of MnNPs. The IC₅₀ of MnNPs was 341, 197, and 219 $\mu\text{g/mL}$ against KATOIII, NCI-N87, and SNU-16 cell lines, respectively. The MnNPs showed the best antioxidant activities against DPPH. It seems that the anti-human gastric cancer effect of recent nanoparticles is due to their antioxidant effects.

Funding

This work was supported by grants from Nn10PY2017-03 program of Harbin Medical University Cancer Hospital. Medical Wisdom Research Fund by the Heilongjiang Sunshine Health Foundation (H21L0806) and China primary health care foundation.

Declaration of Competing Interest

The authors declare that they have no known competing financial interests or personal relationships that could have appeared to influence the work reported in this paper.

References

- Adham, A.N., Naqishbandi, A.M., Efferth, T., 2021. Cytotoxicity and apoptosis induction by *Fumaria officinalis* extracts in leukemia and multiple myeloma cell lines. *J. Ethnopharmacol.* 266, 113458.

- Ahmad, M.B., Lim, J.J., Shameli, K., Ibrahim, N.A., Tay, M.Y., 2011. *Molecules* 16, 7237–7248.
- Allen, T.M., 2002. Ligand-targeted therapeutics in anticancer therapy. *Nat. Rev. Cancer* 2 (10), 750–763.
- Andersson Trojer, M., Li, Y.e., Wallin, M., Holmberg, K., Nydén, M., 2013. Charged microcapsules for controlled release of hydrophobic actives Part II: surface modification by LbL adsorption and lipid bilayer formation on properly anchored dispersant layers. *J. Colloid Interface Sci.* 409, 8–17.
- Arunachalam, K.D. et al., 2003. One-step green synthesis and characterization of leaf extract-mediated biocompatible silver and gold nanoparticles from *Mimosa pudica*. *Int. J. Nanomed.* 8, 1307–1315.
- Beheshtkhou, Nasrin, Kouhbanani, Mohammad Amin Jadidi, Savardashtaki, Amir, Amani, Ali Mohammad, Taghizadeh, Saeed, 2018. Green synthesis of iron oxide nanoparticles by aqueous leaf extract of *Daphne mezereum* as a novel dye removing material. *Appl. Phys. A* 124 (5). <https://doi.org/10.1007/s00339-018-1782-3>.
- Borm, P.J., Robbins, D., Haubold, S., et al., 2006. The potential risks of nanomaterials: a review carried out for ECETOC. *Particle Fibre Toxicol.* 3 (1), 11.
- Byrne, J.D., Betancourt, T., Brannon-Peppas, L., 2008. Active targeting schemes for nanoparticle systems in cancer therapeutics. *Adv. Drug Del. Rev.* 60 (15), 1615–1626.
- Cakić, M., Glišić, S., Cvetković, D., Cvetinović, M., Stanojević, L., Danilović, B., Cakić, K., 2018. Green synthesis, characterization and antimicrobial activity of silver nanoparticles produced from *Fumaria officinalis* L. plant extract. *Colloid J.* 80, 803–813.
- Celardo, I., Pedersen, J.Z., Traversa, E., Ghibelli, L., 2011. Pharmacological potential of cerium oxide nanoparticles. *Nanoscale* 3 (4), 1411–1420.
- Davis, Mark E., Chen, Zhuo, Shin, Dong M., 2008. Nanoparticle therapeutics: an emerging treatment modality for cancer. *Nat Rev Drug Discov.* 7 (9), 771–782.
- De Jong, W.H., Borm, P.J., 2008. Drug delivery and nanoparticles: applications and hazards. *Int. J. Nanomed.* 3 (2), 133–149.
- Deshpande, Pranali P., Biswas, Swati, Torchilin, Vladimir P., 2013. Deshpande, Current trends in the use of liposomes for tumor targeting. *Nanomedicine* 8 (9), 1509–1528.
- Gao, Zhonggao, Lukyanov, Anatoly N., Singhal, Anurag, Torchilin, Vladimir P., 2002. Diacyllipid-polymer micelles as nanocarriers for poorly soluble anticancer drugs. *Nano Lett.* 2 (9), 979–982.
- Gao, J., Wang, Z., Liu, H., Wang, L., Huang, G., 2015. Liposome encapsulated of temozolomide for the treatment of glioma tumor: preparation, characterization and evaluation. *Drug Discov Ther.* 9 (3), 205–212.
- Golchinvafo, A., Anijdan, S.M., Sabzi, M., Sadeghi, M., 2020. The effect of natural inhibitor concentration of *Fumaria officinalis* and temperature on corrosion protection mechanism in API X80 pipeline steel in 1 M H₂SO₄ solution. *Int. J. Press. Vessels Pip.* 188, 104241.
- Guilbert, S., Gontard, N., Gorris, L.G.M., 1996. Prolongation of the shelf-life of perishable food products using biodegradable films and coatings. *LWT-Food Sci Technol.* 29 (1-2), 10–17.
- Itani, R., Al Faraj, S.A., 2019. siRNA Conjugated Nanoparticles-A Next Generation Strategy to Treat Lung Cancer. *Int. J. Mol. Sci.* 20 (23), 6088.
- Kamran, Urooj, Bhatti, Haq Nawaz, Iqbal, Munawar, Jamil, Saba, Zahid, Muhammad, 2019. Biogenic synthesis, characterization and investigation of photocatalytic and antimicrobial activity of manganese nanoparticles synthesized from *Cinnamomum verum* bark extract. *J. Mol. Struct.* 1179, 532–539.
- Katata-Seru, Lebogang, Moremedi, Tshepiso, Aremu, Oluwole Samuel, Bahadur, Indra, 2018. Green synthesis of iron nanoparticles using Moringa oleifera extracts and their applications: Removal of nitrate from water and antibacterial activity against *Escherichia coli*. *J. Mol. Liq.* 256, 296–304.
- Kiasat, R.A., Mouradezagun, A., Saghanzhad, J.S., 2013. *J. Serb. Chem. Soc.* 78, 469–476.
- Li YN, G F. Recent progress in doxorubicin nano-drug delivery systems for reserving multidrug resistance. 2014; 11(3):177-181.
- Liu, D., Chen, L.i., Jiang, S., Zhu, S., Qian, Y., Wang, F., Li, R., Xu, Q., 2014. Formulation and characterization of hydrophilic drug diclofenac sodium-loaded solid lipid nanoparticles based on phospholipid complexes technology. *J. Liposome Res.* 24 (1), 17–26.
- Lu, Y., Wan, X., Li, L., Sun, P., Liu, G., 2021. Synthesis of a reusable composite of graphene and silver nanoparticles for catalytic reduction of 4- nitrophenol and performance as anti-colorectal carcinoma. *J. Mater. Res. Technol.* 12, 1832–1843.
- Mahdavi, B., Paydarfard, S., Zangeneh, M.M., Goorani, S., Seydi, N., Zangeneh, A., 2020. Assessment of antioxidant, cytotoxicity, antibacterial, antifungal, and cutaneous wound healing activities of green synthesized manganese nanoparticles using *Ziziphora clinopodioides* Lam leaves under in vitro and in vivo condition. *Appl. Organomet. Chem.* 34 (1). <https://doi.org/10.1002/aoc.v34.110.1002/aoc.5248>.
- Mao, B.-H., Tsai, J.-C., Chen, C.-W., Yan, S.-J., Wang, Y.-J., 2016. Mechanisms of silver nanoparticle-induced toxicity and important role of autophagy. *Nanotoxicol.* 10 (8), 1021–1040.
- Matsumura, Y., Hamaguchi, T., Ura, T., Muro, K., Yamada, Y., Shimada, Y., Shirao, K., Okusaka, T., Ueno, H., Ikeda, M., et al., 2004., Phase I clinical trial and pharmacokinetic evaluation of NK911, a micelle-encapsulated doxorubicin. *Br. J. Cancer* 91, 1775–1781.
- Mi, F.L., 2005. *Biomacromolecules* 6, 975–987.
- Miller, K.S., Krochta, J.M., 1997. Oxygen and aroma barrier properties of edible films: a review. *Trends Food Sci Tech.* 8 (7), 228–237.
- Mohammed, M.I., Makky, A.M., Teaima, M.H., Abdellatif, M.M., Hamzawy, M.A., Khalil, M.A., 2016. Transdermal delivery of vancomycin hydrochloride using combination of nano-ethosomes and iontophoresis: in vitro and in vivo study. *Drug Deliv.* 23 (5), 1558–1564.
- Namvar, F., Rahman, H.S., Mohamad, R., et al., 2014. Cytotoxic effect of magnetic iron oxide nanoparticles synthesized via seaweed aqueous extract. *Int. J. Nanomed.* 19, 2479–2488.
- Nie, S., Xing, Y., Kim, G.J., Simons, J.W., 2007. Nanotechnology applications in cancer. *Annu. Rev. Biomed. Eng.* 9, 257–288.
- Patra, J.K., Das, G., Fraceto, L.F., Campos, E.V.R., Rodriguez-Torres, M.D.P., Acosta-Torres, L.S., Diaz-Torres, L.A., Grillo, R., Swamy, M.K., Sharma, S., Habtemariam, S., Shin, H.-S., 2018. Nano based drug delivery systems: Recent developments and future prospects. *J. Nanobiotechnol.* 16 (1). <https://doi.org/10.1186/s12951-018-0392-8>.
- Petrućzynik, A., Plech, T., Tuzimski, T., Misiurek, J., Kaproń, B., Misiurek, D., Szultka-Młyńska, M., Buszewski, B., Waksmundzka-Hajnos, M., 2019. Determination of selected isoquinoline alkaloids from *Mahonia aquifolia*; *Meconopsis cambrica*; *Corydalis lutea*; *Dicentra spectabilis*; *Fumaria officinalis*; *Macleaya cordata* extracts by HPLC-DAD and comparison of their cytotoxic activity. *Toxins* 11, 575.
- Radini, Ibrahim Ali, Hasan, Nazim, Malik, Maqsood Ahmad, Khan, Zaheer, 2018. Biosynthesis of iron nanoparticles using *Trigonella foenum-graecum* seed extract for photocatalytic methyl orange dye degradation and antibacterial applications. *J. Photochem. Photobiol.* B 183, 154–163.
- Sangami, S., Manu, M., 2017. Synthesis of Green Iron Nanoparticles using Laterite and their application as a Fenton-like catalyst for the degradation of herbicide Ametryn in water. *Environ. Technol. Innov.* 8, 150–163.
- Sankar, Renu, Maheswari, Ramasamy, Karthik, Selvaraju, Shiva-shangari, Kanchi Subramanian, Ravikumar, Vilwanathan, 2014. Anticancer activity of *Ficus religiosa* engineered copper oxide nanoparticles. *Mat. Sci. Eng. C* 44, 234–239.

- Sharef, A.Y., Aziz, F.M., Adham, A.N., 2020. The protective effect of *Fumaria officinalis* against the testicular toxicity of fluoxetine in rat. *Zanco J. Med. Sci.* 24, 117–131.
- Souri, Mahsa, Hoseinpour, Vahid, Ghaemi, Nasser, Shakeri, Alireza, 2019. Procedure optimization for green synthesis of manganese dioxide nanoparticles by *Yucca gloriosa* leaf extract. *Int. Nano Lett.* 9 (1), 73–81.
- Stapleton, P.A., Nurkiewicz, T.R., 2014. Vascular distribution of nanomaterials. *Wiley Interdiscipl. Rev. Nanomed. Nanobiotechnol.* 6 (4), 338–348.
- Thi, P.P.N., Nguyen, D.H., 2016. *Green Process. Synth.* 5, 467–472.
- Torchilin, Vladimir P., 2007. Targeted pharmaceutical nanocarriers for cancer therapy and imaging. *AAPS J.* 9 (2), E128–E147.
- Xinli, D.H.Z.S., 2012. Applications of nanocarriers with tumor molecular targeted in chemotherapy. *Chemistry.* 75 (7), 621–627.
- Yang, F., Jin, C., Jiang, Y., Li, J.i., Di, Y., Ni, Q., Fu, D., 2011. Liposome based delivery systems in pancreatic cancer treatment: from bench to bedside. *Cancer Treat. Rev.* 37 (8), 633–642.
- You, C., Han, C., Wang, X., Zheng, Y., Li, Q., Hu, X., Sun, H., 2012. The progress of silver nanoparticles in the antibacterial mechanism, clinical application and cytotoxicity. *Mol. Biol. Rep.* 39 (9), 9193–9201. <https://doi.org/10.1007/s11033-012-1792-8>.
- Zhang, Y., Huang, Y., Li, S., 2014. Polymeric micelles: Nanocarriers for cancer-targeted drug delivery. *AAPS PharmSciTech* 15, 862–871.